

Empirical rules for rationalising visible circular dichroism of Cu^{2+} and Ni^{2+} histidine complexes: Applications to the prion protein

Mark Klewpatinond, John H. Viles*

School of Biological and Chemical Sciences, Queen Mary, University of London, Mile End Road, London E1 4NS, UK

Received 7 February 2007; revised 27 February 2007; accepted 27 February 2007

Available online 6 March 2007

Edited by Gianni Cesareni

Abstract A natively unfolded region of the prion protein, PrP(90–126) binds Cu^{2+} ions and is vital for prion propagation. Pentapeptides, acyl-GGGTH^{92–96} and acyl-TNMKH^{107–111}, represent the minimum motif for this Cu^{2+} binding region. EPR and ¹H NMR suggests that the coordination geometry for the two binding sites is very similar. However, the visible CD spectra of the two sites are very different, producing almost mirror image spectra. We have used a series of analogues of the pentapeptides containing His⁹⁶ and His¹¹¹ to rationalise these differences in the visible CD spectra. Using simple histidine-containing tri-peptides we have formulated a set of empirical rules that can predict the appearance of Cu^{2+} visible CD spectra involving histidine and amide main-chain coordination.

© 2007 Federation of European Biochemical Societies. Published by Elsevier B.V. All rights reserved.

Keywords: CD; Spectroscopy; Metals; Copper; Coordination; Complex

1. Introduction

The application of circular dichroism (CD) spectroscopy in the far and near UV is well documented. However, although Lifshitz reported the cotton effect associated with metal ions in 1925, the interpretation of visible CD associated with metal binding is not so well understood. Visible CD spectroscopy can be a very powerful technique to study metal–protein interactions and has gained a resurgence of interest in recent years [1–15]. Absorption bands from d–d electronic transitions are often broad and featureless, and these bands can consist of two or more overlapping bands, produced by different d–d electron transitions. For example, the absorption maxima observed for Cu^{2+} square-planar complexes result from three overlapping transitions [16]. These different bands are often not fully resolved in the absorption spectra, but CD spectroscopy can resolve the individual transitions as separate bands, particularly where the CD bands are of opposite sign. Consequently, CD bands do not always correspond to the wavelength of the observed absorption maxima. Unlike absorption spectra, CD spectra are only produced where a me-

tal ion is in a chiral environment, thus, the free metal ion d–d transitions are typically CD silent. In this way, the use of visible CD has the advantage of being immune from interference by free metal ions, as only the protein-bound species are observed. Thus, pH dependence, stoichiometry and metal binding curves are readily generated [1]. Furthermore, non-chiral competing ligands can aid in affinity measurements [2,3].

Optical activity in transition metal ion complexes have been attributed to three sources: the configurational effect; the conformational effect and the vicinal effect [17,18]. The configurational effect makes the strongest contribution to optical activity and occurs when the distribution of donor groups or atoms coordinated to the metal ion is not symmetrical. The conformational effect is due to ring puckering occurring with certain combinations of ligands and metal ions [19]. In tetragonal peptide complexes with Cu^{2+} , Pd^{2+} and low spin Ni^{2+} in which coordination tends to be planar, the main determinant of optical activity is the vicinal effect arising from the chiral substituents around the chelate ring [17,18]. Relatively strong CD bands are often observed for d–d transitions of tetragonal complexes involving backbone amide and histidine coordination, via the imidazole ring [1–13]. Here, the optical activity observed is due to the vicinal contributions resulting when the chiral alpha carbon is held in a chelate ring between two chelating donor atoms, typically adjacent main-chain amides [18]. The position of the amino acids around the coordination plane modulates the vicinal effect. A set of section rules was devised to describe this effect. The hexadecant rule divides the space around the metal ion into 16 quadrants with alternating sign, while the position of side-chains within these 16 quadrants dictates the sign of the contribution [17,18]. However, the sector rule is not applicable to histidine containing complexes, which represent the majority of Cu^{2+} complexes bound to main-chain amides with appreciable affinity. Thus, the hexadecant rule is rather cumbersome and its applications limited. Here, we aim to derive a set of empirical rules for predicting the appearance of visible CD spectra for Cu^{2+} and Ni^{2+} square-planar complexes involving histidine and main-chain coordination.

2. Materials and methods

2.1. Peptide synthesis and purification

F-moc chemistry was used to synthesise various fragments of prion protein (PrP). All peptides used were N-terminally acetylated and C-terminally amidated in order to mimic this region of PrP within the full-length protein (A.B.C., Imperial College, London). The peptides were removed from the resin and de-protected before purification by reverse-phase HPLC. The samples were characterised using mass

*Corresponding author. Fax: +44 020 8983 0973.
E-mail address: j.viles@qmul.ac.uk (J.H. Viles).

Abbreviations: CD, circular dichroism; PrP, prion protein; NMR, nuclear magnetic resonance; EPR, electron paramagnetic resonance; His, histidine

spectrometry and ^1H NMR spectroscopy. Peptides included: PrP(92–96) GGGTH; PrP(107–111) TNMKH; PrP(110–115) KHMAGA. Pentapeptide analogues synthesised also included: TNMAH; TNAKH; TAMKH; TNGKH; GGGAH and GGATH. In addition four tripeptides GGH; GAH; AGH and AAH were synthesised.

2.2. Titrations

Small aliquots of fresh aqueous solutions were used to add metal ions (Cu^{2+} as $\text{CuCl}_2 \cdot 2\text{H}_2\text{O}$, Ni^{2+} as $\text{NiCl}_2 \cdot 6\text{H}_2\text{O}$). All titrations were carried out in the absence of buffers and the pH was measured before and after acquiring each spectrum, adjusting the pH when necessary using small aliquots of 100 mM NaOH or HCl. Peptide concentrations were calculated using the dried weight of each peptide, assuming 10% moisture content for all peptides.

2.3. Circular dichroism (CD)

CD spectra were recorded on an Applied Photophysics Chirascan instrument at 25 °C. A cell with a 1 cm pathlength was used for spectra recorded between 300 and 800 nm, with sampling points every 2 nm. Typically, four scans were recorded, and baseline spectra were subtracted from each spectrum. Data were processed using Applied Photophysics Chirascan Viewer, Microsoft Excel and the Kaleida-Graph spreadsheet/graph package, smoothing of data were not required. The direct CD measurements (θ , in millidegrees) were converted to molar ellipticity, $\Delta\epsilon$ ($\text{M}^{-1}\text{cm}^{-1}$), using the relationship $\Delta\epsilon = \theta/33000 \cdot c \cdot l$, where c is the molar concentration and l is the pathlength.

2.4. Electron paramagnetic resonance spectroscopy (EPR)

X-band EPR spectra were acquired on a Bruker Elexsys E500 spectrometer operating at a microwave frequency of 9.33 GHz. The spectra were acquired over a sweep width of 2000 G, modulation amplitude of 20 G, and a temperature of ~ 20 K.

2.5. Proton nuclear magnetic resonance (NMR)

^1H NMR spectra were acquired at 296 K on a Varian Unity 600 MHz spectrometer using 5 mm inverse-detection (^1H), triple resonance, z-gradient probes. Spectra were recorded in 100% D_2O , a low power pre-saturation pulse was used to suppress residual water. TOCSY spectra were typically acquired with $2048[\text{F}2] \times 512[\text{F}1]$ complex points, employing a DIPSI2 sequence for isotropic mixing, with a mixing time of ~ 60 ms. The States-TPPI method was used for quadrature detection in the indirect dimension for 2D spectra. Prior to Fourier transformation, sine-squared window functions, phase shifted by 90° , were applied to both dimensions and zero filled to 2048 real points. Data were processed and analysed using V_{nmr} (Varian) software running on a SGI O2. Proton resonance assignments of each pentapeptide were obtained using the 2D TOCSY data.

3. Results and discussion

We became particularly interested in the source of the sign modulation of the visible CD spectra associated with the metal d–d transitions when we observed Cu^{2+} (and Ni^{2+}) binding centred around His^{96} or His^{111} for a number of prion protein fragments [4,24]. It is interesting to note that the CD bands for both the Ni^{2+} and Cu^{2+} complexes incorporating His^{96} are positive to shorter wavelengths of the absorption maximum (~ 540 nm for Cu^{2+} and ~ 440 nm for Ni^{2+}) and negative to longer wavelengths. In contrast the CD bands for both Cu^{2+} and Ni^{2+} complexes at His^{111} produce negative CD bands to shorter wavelengths and positive to longer wavelengths. Thus, the complexes give visible CD spectra that are almost mirror images of each other as shown for the pentapeptides, PrP(92–96) and PrP(107–111) in Fig. 1. The differences causing these mirror-image CD spectra must be subtle, as ^1H NMR and EPR suggest almost identical coordination. Both Cu^{2+}

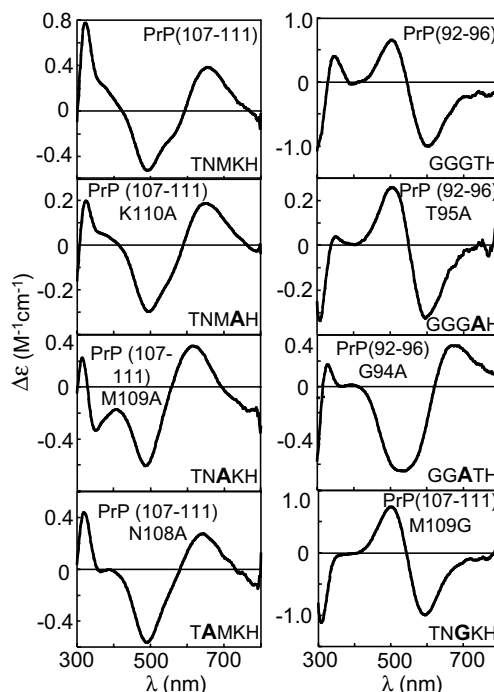


Fig. 1. Visible CD spectra of Cu^{2+} bound to various analogues of PrP(92–96) and PrP(107–111). Using 1 mole equivalent Cu^{2+} at pH 7.8 and 0.1 mM peptide. All peptides are acetylated at the N-terminus and amidated at the C-terminus.

and Ni^{2+} bind to His^{96} and His^{111} independently of each other, forming a similar 4N square-planar complex, shown in Fig. 2.

Cu^{2+} -EPR spectra make no distinction between the two Cu^{2+} pentapeptide complexes forming a Type II axial complex, Fig. 3. At pH 7.8 and 9, the A_{\parallel} and g_{\parallel} values are consistent with a 4N species, with A_{\parallel} and g_{\parallel} values of 16.5 mK and 2.27, respectively. At pH 6, the g_{\parallel} value shifts to higher field and the hyper-fine splitting reduces, which is more typical of a 3N1O species with A_{\parallel} and g_{\parallel} values of 15.3 mK and 2.29. The pH dependence of the Cu^{2+} coordination is also apparent from the visible CD spectra. At pH 6, a weak positive CD band is observed at 530 nm assigned to the 3N1O species [24], while the spectra shown in Fig. 1 are for the 4N complex, which dominate at pH values above 7. Elsewhere, we have

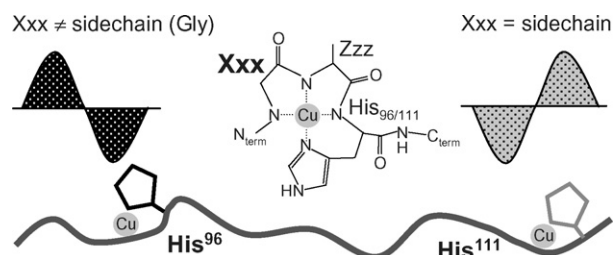


Fig. 2. Schematic of the square-planar metal binding sites at His^{96} and His^{111} of the prion protein and associated visible CD signal. This is a 4N complex that dominates at pH ~ 7 and above. Zzz represents Thr 95 or Lys 110 , Xxx represents Gly 94 or Met 109 . Cu^{2+} or Ni^{2+} binding at His^{96} , with a Gly two residues preceding the histidine, produces the visible CD spectra illustrated in black. Conversely binding at His^{111} , with a side-chain in the Xxx position, produces the mirror image visible CD spectra illustrated in grey.

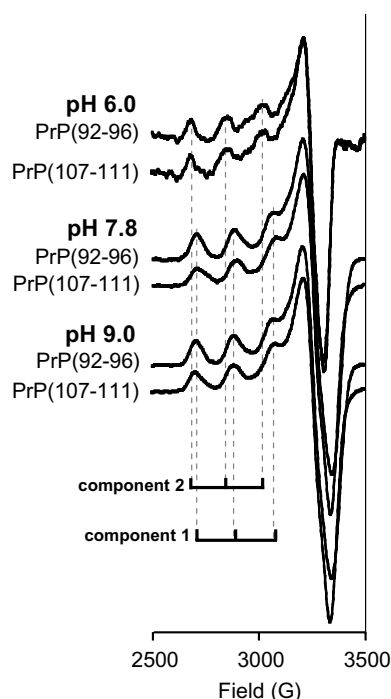


Fig. 3. EPR spectra CuIPrP(92–96) and CuIPrP(107–111) at pH 6.0, pH 7.8 and pH 9.0. Recorded at 20 K and peptide concentrations of 0.1 mM.

shown that these complexes form 1:1 species under these conditions: 0.1 mM peptide, stoichiometric metal ion, pH > 7 [4] while lower pH and sub-stoichiometric copper may favour a 2:1 peptide:copper complex [24]. Similarly, ^1H NMR studies (see Fig. 4 and Ref. [4]) pH 9 of Ni^{2+} binding for both pentapeptides, PrP(92–96) and PrP(107–111), show a single diamagnetic low-spin square-planar complex formed with a 1:1 stoichiometry, characteristic of a 4N complex [4].

We first postulated that the difference in the visible CD spectra might be due to the direction of the main-chain coordination N or C terminal from the His residues, as had been previously suggested [12]. However, our studies with pentapeptides indicate that the metal ion is binding N-terminally from the His residue. A hexapeptide with residues C-terminal of the His, PrP(110–115), KHMAGA, does not bind Cu^{2+} or Ni^{2+} with the same coordination.

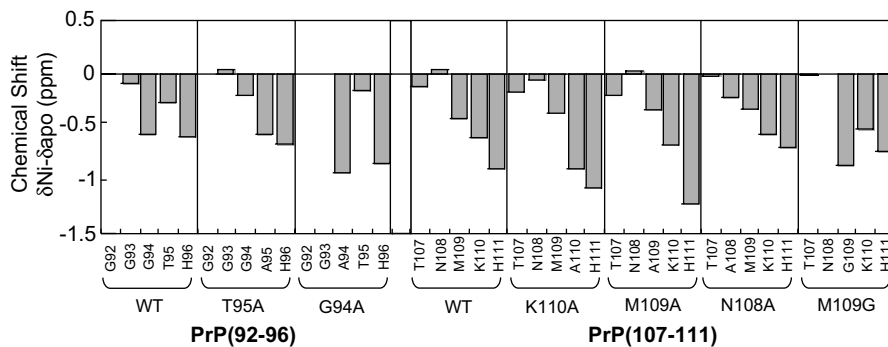


Fig. 4. ^1H NMR chemical shifts for α protons upon Ni^{2+} coordination for pentapeptides and analogues. Ni^{2+} -induced coordination shifts are for the Hz of each residue in PrP(92–96), PrP(107–111) and their analogues at pH 9.0. Peptide concentrations of 0.5 mM.

Then we proposed that axial coordination of the side-chain group Lys ϵNH_3 , Met ϵS or Asn NH_3 group within TNMKH, not present in the GGGTH peptide, might be the source of the difference in circular dichroism. However, mutation of each of these in turn: TNMAH; TNAKH; TAMKH had no effect on the sign of the circular dichroism as shown in Fig. 1. Then, we postulated that the difference in circular dichroism could arise from axial coordination of the Thr hydroxyl group in the PrP(92–96) pentapeptide. Again, substitution of Thr⁹⁵ to an Ala residue had little effect on the CD spectra, Fig. 1. Finally, we decided it must be the presence or absence of a side-chain that conferred the difference in the two complexes. Substitution of a Gly for an Ala in PrP(92–96) had a dramatic effect, reversing the CD spectra observed, Fig. 1. Similarly, the opposite effect can be achieved with PrP(107–111) by replacing the Met with Gly rather than Ala, thus, inverting the circular dichroism signal. The presence of a side-chain Ala or Met at the second residue preceding the His gives a negative band to shorter wavelengths. While the presence of a Gly at this position produces a positive CD band to shorter wavelengths.

When modelling different side-chain substitution preceding the His residue for the 4N complex it is clear that the Ala to Gly substitution will not significantly affect the Cu^{2+} coordination geometry of the complex. ^1H NMR was used to confirm that the 4N coordination geometry is unaffected in the pentapeptide analogues used. Fig. 4 shows coordination shifts upon Ni^{2+} binding for the various peptides. The Hz shifts have been compared for the wild-type pentapeptides, PrP(92–96) and PrP(107–111), to that of the accompanying analogues. The data confirm that the substitutions do not affect the basic 4N coordination, including, His ϵN and three amides of the Histidine and the two preceding residues. All analogues studied produce the same diamagnetic low-spin square-planar complex with Ni^{2+} . There are characteristic changes in the alpha proton chemical shifts. Residues involved in direct amide coordination all exhibit coordination shifts to high-field typically between 0.3 and 0.9 ppm, upon Ni^{2+} binding.

To test our rationale for predicting the appearance of the visible CD spectra for histidine-containing peptides, we decided to investigate the phenomenon of the inverted CD signal more fully using the more general case of simple model tripeptides acetylated at the N-terminus. Four tri-peptides were produced: GGH, AGH, GAH and AAH. Visible CD spectra obtained with 1 mole equivalent of Cu^{2+} bound at pH 9.5 are shown in Fig. 5. The spectra are obtained at pH 9.5 to en-

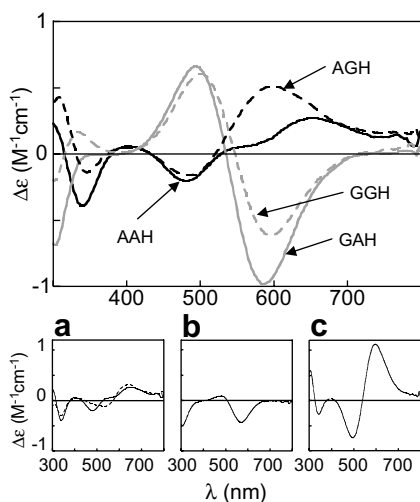


Fig. 5. Visible CD spectra Cu^{2+} bound to AAH, GAH, AGH and GGH. All peptides are N-terminally acetylated with 1 mole equivalent of Cu^{2+} added at pH 9.5, peptide concentrations of 0.1 mM. Inset panels show simulated additions of spectra of (a) Cu_1AAH (solid line) overlaid with $(\text{Cu}_1\text{AGH} + \text{Cu}_1\text{GAH} - \text{Cu}_1\text{GGH})$, (b) $\text{Cu}_1\text{GAH} - \text{Cu}_1\text{GGH}$, and (c) $\text{Cu}_1\text{AGH} - \text{Cu}_1\text{GGH}$.

sure that the 4N species dominates, rather than a 3N1O complex. The four Cu^{2+} loaded peptide spectra obtained at pH 9.5 give CD bands as were predicted by the studies on the pentapeptide analogues of PrP described in Fig. 1. In particular, the visible CD signal is clearly modulated by the presence of Ala or Gly at the position two residues preceding the His residue.

Contributions of the side-chain to the CD signal should be additive, so to test this we carried out simple additions/subtractions to simulate related spectra. As Gly residues should not contribute to the CD signal, then Cu^{2+} loaded spectra of $\text{AGH} + \text{GAH} - \text{GGH}$ should have the appearance of Cu^{2+} loaded spectra of AAH. The simulated spectrum is overlaid with the Cu-AAH spectrum. Comparison of the two spectra, Fig. 5a, shows a close similarity in terms of position and intensity of bands. Furthermore, $\text{GAH} - \text{GGH}$ gives a spectrum that simulates the contribution of Ala one residue preceding the His residue, (Fig. 5b). As predicted from the pentapeptide studies (Fig. 1), this signal is quite weak and has only a small contribution on the overall spectra. Most striking is the spectra of $\text{AGH} - \text{GGH}$, which gives a spectrum that simulates the contribution of a side-chain two residues preceding the His. As predicted by the pentapeptide analogues, the presence of Ala two residues preceding the His has a sizeable contribution to the visible CD spectra with a relatively intense negative CD band at 480 nm and an intense positive band at 600 nm, Fig. 5c. The CD bands produced are of opposite sign to that of the histidine residue contribution alone (GGH) and are of greater intensity. The strength of the CD is sufficiently intense to invert the sign of the overall spectra. Thus, we have a prediction that Cu^{2+} (or Ni^{2+}) binding to His-containing proteins or peptides to form 4N complexes, will result in a CD spectrum with positive CD to shorter wavelengths and negative to longer wavelengths for GZH peptides (where Z can be any primary amino acid). While XZH (where X can be any amino acid, except Gly or Pro) will result in a negative CD signal to shorter wavelengths and a positive CD signal to longer wavelengths.

We have surveyed the publications of visible CD spectra for His-containing Cu^{2+} complexes to see if these rules can be applied to other copper-histidine complexes. The application of these simple predictive rules are confirmed for peptides with a single histidine. For example, as predicted the Cu^{2+} AcGGGH and AcGGHG visible CD spectra [12] have the striking appearance of PrP(92–96), while the Cu-AcELAKHA peptide [13] has the appearance of PrP(107–111), as expected. Papers by Mylonas et al. show the Cu^{2+} and Ni^{2+} 4N complexes for the peptide AcTESHAK [20,21], and as predicted, these Ni^{2+} and Cu^{2+} complexes have a very similar appearance to PrP(107–111). A related peptide, AcTESAHK, has a more complicated behaviour [21]; however, the spectra predicted by our empirical rule can readily be created by simply subtracting out the contribution to the spectra for the intermediate species, which dominates at pH 6, from the 4N pH 10 spectra. Complexes involving multiple histidines [22,23] or a free amino group [6,9] do not produce the complex shown in Fig. 2 and do not have the appearance of the visible CD spectra shown here. In peptides and unstructured proteins containing a His residue, a common coordination mode is that of the 4N complex described for His⁹⁶ and His¹¹¹ of the prion protein. Coordination of amides to the C-terminal of the His will take place if a Pro precedes the His, as is evident for the octarepeat region of PrP. In this case, the visible CD spectra have quite a different appearance [1,2]. We hope that our empirical rules will help in the interpretation of visible CD spectra for Cu^{2+} and Ni^{2+} square-planar complexes.

Acknowledgements: This work was funded by BBSRC Project Grants and Studentship. Thanks to the NIMR for use of NMR facilities as well as S. Rigby, C. Jones and A. Garnett.

References

- [1] Viles, J.H., Cohen, F.E., Prusiner, S.B., Goodin, D.B., Wright, P.E. and Dyson, J.H. (1999) Copper binding to the prion protein: structural implications of four identical cooperative binding sites. *Proc. Natl. Acad. Sci. USA* 96, 2042–2047.
- [2] Garnett, A.P. and Viles, J.H. (2003) Copper binding to the octarepeats of the prion protein. Affinity, specificity, folding, and cooperativity: insights from circular dichroism. *J. Biol. Chem.* 278, 6795–6802.
- [3] Jones, C.E., Abdelraheim, S.R., Brown, D.R. and Viles, J.H. (2004) Preferential Cu^{2+} Coordination by His⁹⁶ and His¹¹¹ Induces $\{\beta\}$ -sheet formation in the unstructured amyloidogenic region of the prion protein. *J. Biol. Chem.* 279, 32018–32027.
- [4] Jones, C.E., Klewpatinond, M., Abdelraheim, S.R., Brown, D.R. and Viles, J.H. (2005) Probing copper²⁺ binding to the prion protein using diamagnetic nickel²⁺ and 1H NMR: the unstructured N terminus facilitates the coordination of six copper²⁺ ions at physiological concentrations. *J. Mol. Biol.* 346, 1393–1407.
- [5] Wells, M.A., Jelinska, C., Hosszu, L.L., Craven, C.J., Clarke, A.R., Collinge, J., Waltho, J.P. and Jackson, G.S. (2006) Multiple forms of copper(II) coordination occur throughout the disordered N-terminal region of the prion protein at pH 7.4. *Biochem. J.* 400, 501–510.
- [6] Bal, W., Christodoulou, J., Sadler, P.J. and Tucker, A. (1998) Multi-metal binding site of serum albumin. *J. Inorg. Biochem.* 70, 33–39.
- [7] Pappalardo, G., Imperlizzeri, G., Bonomo, R.P., Campagna, T., Grasso, G. and Saita, M.G. (2002) Copper(II) and nickel(II) binding modes in a histidine-containing model dodecapeptide. *New J. Chem.* 26, 593–600.
- [8] Boka, B., Myari, A., Sovago, I. and Hadjiliadis, N. (2004) Copper(II) and zinc(II) complexes of the peptides Ac-HisValHis-

- NH₂ and Ac-HisValGlyAsp-NH₂ related to the active site of the enzyme CuZnSOD. *J. Inorg. Biochem.* 98, 113–122.
- [9] Conato, C., Kozłowski, H., Swiatek-Kozłowska, J., Mlynarz, P., Remelli, M. and Silvestri, S. (2004) Formation equilibria of nickel complexes with glycyl-histidyl-lysine and two synthetic analogues. *J. Inorg. Biochem.* 98, 153–160.
- [10] Jozsai, V., Nagy, Z., Osz, K., Sanna, D., Di Natale, G., La Mendola, D., Pappalardo, G., Rizzarelli, E. and Sovago, E. (2006) Transition metal complexes of terminally protected peptides containing histidyl residues. *J. Inorg. Biochem.* 100, 1399–1409.
- [11] Kallay, C., Varnagy, K., Malandrinos, G., Hadjiliadis, N., Sanna, D. and Sovago, I. (2006) Copper(II) complexes of terminally protected pentapeptides containing three histidyl residues in alternating positions, Ac-His-Xaa-His-Yaa-His-NH₂. *Dalton Trans.* 38, 4545–4552.
- [12] Orfei, M., Alcaro, M.C., Marcon, G., Chelli, M., Ginanneschi, M., Kozłowski, H., Brasun, J. and Messori, L. (2003) Modeling of copper(II) sites in proteins based on histidyl and glycyl residues. *J. Inorg. Biochem.* 97, 299–307.
- [13] Karavelas, T., Mylonas, M., Malandrinos, G., Plakatouras, J.C., Hadjiliadis, N., Mlynarz, P. and Kozłowski, H. (2005) Coordination properties of Cu(II) and Ni(II) ions towards the C-terminal peptide fragment -ELAKHA- of histone H2B. *J. Inorg. Biochem.* 99, 606–615.
- [14] Brasun, J., Gabbiani, C., Ginanneschi, M., Messori, L., Orfei, M. and Swiatek-Kozłowska, J. (2004) The copper(II) binding properties of the cyclic peptide c(HGHK). *J. Inorg. Biochem.* 98, 2016–2021.
- [15] Osz, K., Boka, B., Varnagy, K., Sovago, I., Kurtan, T. and Antus, S. (2002) The application of circular dichroism spectroscopy for the determination of metal ion speciation and coordination modes of peptide complexes. *Polyhedron* 21, 2149–2159.
- [16] Martin, R.B. (1974) (Sigel, H., Ed.), *Metal Ions in Biological Systems*, Vol. 1, pp. 129–156, Marcel Dekker, New York.
- [17] Martin, R.B., Tsangaris, J.M. and Chang, J.W. (1968) A double octant rule for planar transition metal ion complexes. *J. Am. Chem. Soc.* 90, 821–823.
- [18] Tsangaris, J.M. and Martin, R.B. (1970) Visible circular dichroism of copper(II) complexes of amino acids and peptides. *J. Am. Chem. Soc.* 92, 4255–4260.
- [19] Kuroda, R. and Saito, Y. (2000) in: *Circular Dichroism: Principles and Applications* (Berova, N., Nakanishi, K. and Woody, R.W., Eds.), pp. 563–599, Wiley, New York.
- [20] Mylonas, M., Krezel, A., Plakatouras, J.C., Hadjiliadis, N. and Bal, W. (2002) The binding of Ni(II) ions to terminally blocked hexapeptides derived from the metal binding -ESHH- motif of histone H2A. *Dalton Trans.* 22, 4296–4306.
- [21] Mylonas, M., Plakatouras, J.C., Hadjiliadis, N., Krezel, A. and Bal, W. (2002) Potentiometric and spectroscopic studies of the interaction of Cu(II) ions with the hexapeptides AcT-hrAlaSerHisHisLysNH₂, AcThrGluAlaHisHisLysNH₂, AcT-hrGluSerAlaHisLysNH₂ and AcThrGluSerHisAlaLysNH₂, models of C-terminal tail of histone H2A. *Inorg. Chim. Acta* 339, 60–70.
- [22] Bal, W., Lukszo, J., Bialkowski, K. and Kasprzak, K.S. (1998) Interactions of Nickel(II) with histones: interactions of Nickel(II) with CH₃CO-Thr-Glu-Ser-His-His-Lys-NH₂, a peptide modeling the potential metal binding site in the “C-Tail” region of histone H2A. *Chem. Res. Toxicol.* 11, 1014–1023.
- [23] Syme, C.D., Nadal, R.C., Rigby, S.E. and Viles, J.H. (2004) Copper binding to the amyloid-beta (Aβ) peptide associated with Alzheimer’s disease: folding, coordination geometry, pH dependence, stoichiometry, and affinity of Aβ(1–28): insights from a range of complementary spectroscopic techniques. *J. Biol. Chem.* 279, 18169–18177.
- [24] Klewpatinond, M. and Viles, J.H. (2007) Fragment length influences affinity for Copper²⁺ and Nickel²⁺ binding to His₉₆ and His₁₁₁ of the prion protein and spectroscopic evidence for a multiple His binding only at low pH. *Biochem. J.*, doi:10.1042/BJ20061893.